Frascati Physics Series Vol. LVI (2012)
Dark Forces at Accelerators
October 16-19, 2012

SEARCH FOR DARK SECTOR AT BESIII

Jinlin FU (for the BESIII Collaboration)
Department of Physics, Nanjing University, China

Abstract

With 106M ψ' events collected at BESIII detector, there is no observed signal of light Higgs-like boson A^0 in process $J/\psi \to \gamma A^0$, $A^0 \to \mu^+\mu^-$. The A^0-mass-dependent upper limits at the 90% C.L. of branching fraction for $J/\psi \to \gamma A^0$, $A^0 \to \mu^+\mu^-$ are range from 4×10^{-7} to 2.1×10^{-5}, for M$(A^0) < 3.0$ GeV/c^2. With 225M J/ψ data sample, there is no obseved signal of light dark matter particles or U boson in invisible decays of η and η'. The upper limits at the 90% C.L. are determined to be 2.6×10^{-4} for the ratio $\frac{\mathcal{B}(\eta\to\text{invisible})}{\mathcal{B}(\eta\to\gamma\gamma)}$ and 2.4×10^{-2} for $\frac{\mathcal{B}(\eta'\to\text{invisible})}{\mathcal{B}(\eta'\to\gamma\gamma)}$. These limits may be used to constrain light dark matter particles or spin-1 U bosons.

1 The BEPC-II collider and BES-III detector

BEPCII/BESIII [1)] is a major upgrade of the BESII experiment at BEPC accelerator. The achieved peak luminosity of the double-ring e^+e^- collider,

BEPCII, is 0.65×10^{33} cm^{-2} s^{-1} at energy of $\psi(3770)$. The BESIII detector consists of a main drift chamber with momentum resolution 0.5% at 1 GeV/c, an electromagnetic calorimeter with energy resolution 2.5% at 1 GeV/c and a time-of-flight system inside a superconducting solenoidal magnet with a magnetic strength of 1 T. The magnet is surrounded by the muon system made of resistive plate chambers. Based on data samples of 1.06×10^8 ψ' [2] and 2.25×10^8 J/ψ [3], two analyses are performed for dark sector search.

2 Search for a light exotic particle in $J/\psi \to \gamma\mu^+\mu^-$

The HyperCP experiment [4] obsered three anomalous $\Sigma \to p\mu^+\mu^-$ events with $\mu^+\mu^-$ invariant mass around 214.3 MeV/c^2. A particle with these properties could be the pseudoscalar sgoldstino particle [5] in various supersymmetric models [6], a light pseudoscalar Higgs-like boson A^0 [7], or a vector U boson [8]. No evidence of new physics has been found by studying light dilepton-resonance in $p\bar{p}$ collision, e^+e^- collision and b-quark decays, but it is still important to search for $J/\psi \to \gamma A^0$ to check the possible couples to c-quark and leptons. Theoretically, the branching fraction of $J/\psi \to \gamma A^0$ is about 10^{-9} to 10^{-7} level [9]. The upper limits of branching fraction of $J/\psi \to \gamma A^0$ are set by Crystal Ball experiment which are less than 1.4×10^{-5} (90% C.L.) for $M(A^0) <$ 1.0 GeV/c^2 [10].

The process $\psi' \to \pi^+\pi^- J/\psi$, $J/\psi \to \gamma A^0$, $A^0 \to \mu^+\mu^-$ is used to search for an A^0, and A^0 is assumed as a pseudoscalar (or scalar) particle with narrow width and negligible decay time. Two positive, two negative charged tracks and at least one good photon are required. The events with multiple photons, should be passed through the π^0 veto. The γ with the highest energy is regarded as the photon from J/ψ. The oppositely charged track pair with recoil mass closest to the J/ψ mass is regarded as the π^+ and π^-. The other two charged tracks with at least one satisfying muon identification is assigned as the μ^+ and μ^-. The J/ψ is tagged by constraining $\pi^+\pi^-$ recoil mass within a narrow window. In order to get better mass resolution and suppress backgrounds further, the events are kinematically fitted using energy and momentum conservation constraints under the $\psi' \to \gamma\pi^+\pi^-\mu^+\mu^-$ hypothesis.

The entire $\mu^+\mu^-$ mass range from threshold to 3.0 GeV/c^2 is studied. There is no evidence narrow peak in the mass distribution and only one event with mass of 213.3 MeV/c^2 [shown in Fig.2a]. To set upper limits on the

production rates for different masses, the unbinned maximum-likelihood fits are performed to ∼300 MeV/c^2-wide ranges of the invariant mass spectrum where the mass of the A^0 peak is restricted to be within a series of 5 MeV/c^2-wide intervals near the center of the range. In each fit, the A^0 signal shape is determined from MC simulation, and the background shape is modeled with a polynomial. The limits on the signal yield in each 5 MeV/c^2 interval are set with Bayesian method at the 90% C.L.. Figure1 shows a typical fit to the $\mu^+\mu^-$ invariant mass spectrum in the 5 MeV/c^2-wide interval centred at 2.43 GeV/c^2. The upper limits at the 90% C.L. on the branching fractions of $J/\psi \to \gamma A^0$, $A^0 \to \mu^+\mu^-$ is calculated with

$$\mathcal{B} < \frac{\mathrm{Nsig(UL)}/\epsilon}{\mathrm{N}(\psi') \times \mathcal{B}(\psi' \to \pi^+\pi^-\mathrm{J}/\psi) \times (1-\sigma)}, \tag{1}$$

where Nsig(UL), shown in Fig.2b, is the upper limit on the number of signal events in each M($\mu^+\mu^-$) bin; ϵ is the A^0-mass-dependent selection efficiency determined from MC simulation; N(ψ') is the number of ψ' events; $\mathcal{B}(\psi' \to \pi^+\pi^- J/\psi)$ is set at Particle Data Group (PDG) value [11]; and σ is the total systematic error.

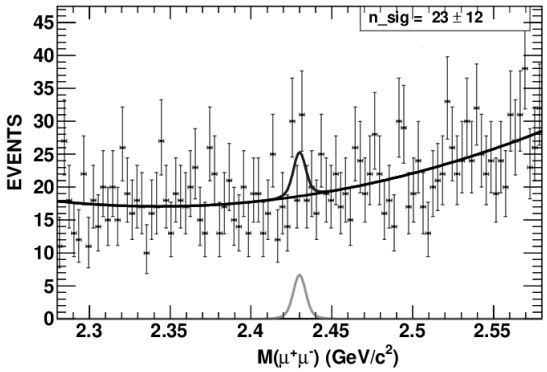

Figure 1: *A typical fit to the invariant-mass spectrum M($\mu^+\mu^-$) in the 5 MeV/c^2 wide interval centered at 2.43 GeV/c^2.*

There is no evidence observed. The A^0-mass-dependent upper limits on the branching fraction for $J/\psi \to \gamma A^0$, $A^0 \to \mu^+\mu^-$ are range from 4×10^{-7} to

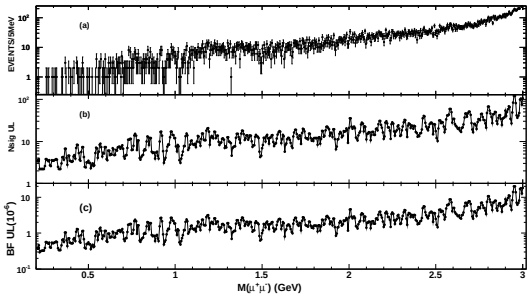

Figure 2: *a) The $\mu^+\mu^-$ invariant mass distribution for the selected $\psi' \to \pi^+\pi^- J/\psi$, $J/\psi \to \gamma\mu^+\mu^-$; b) Upper limits at the 90% C.L. on the number of signal events (Nsig UL) as a function of the $\mu^+\mu^-$ invariant mass; c) Upper limits at the 90% C.L. on the branching fractions (BF UL).*

2.1×10^{-5} [shown in Fig.2c]. Only one event is seen with a $\mu^+\mu^-$ mass of 213.3 MeV/c^2, and the product-branching-fraction upper limit is 5×10^{-7} at the 90% C.L. These limits can rule out much of the parameter space in theoretical models [12].

3 Search for η and $\eta\prime$ invisible decays

Despite of tentative estimation like $\mathcal{B}(\eta(\eta') \to \chi\chi) \approx 1.4\times10^{-4}$ (1.5×10^{-6}) [13], one cannot reliable predict such invisible decay rates of mesons just from the dark matter relic density and annihilation cross section [14]. Due to the U boson vectorially coupled to quarks and leptons [15] and more specific case of the U boson coupled to ordinary particles through the electromagnetic current [16], the annihilation process $q\bar{q} \to UU$ may be also a source of invisible meson decays, especially as the invisible decay mode $U \to \chi\chi$ may be dominant [15]. Invisible decays of η and η' may originate from $\eta(\eta') \to \chi\chi$ or $U_{\rm inv}U_{\rm inv}$. Many searches for invisible decays of π^0, η, η', J/ψ and $\Upsilon(1S)$ have been performed [17, 18, 19, 20, 21]. The resulting data can give constraints on different matrix.

The processes $J/\psi \to \phi\eta$ and $\phi\eta'$ are used to study invisible decays of η and η'. The ϕ can be reconstructed with $\phi \to K^+K^-$ decay model. No charged track is required besides those from $\phi \to K^+K^-$. No neutral track is required

inside a cone of 1.0 rad around the recoil direction against the ϕ candidate. The reconstructed ϕ particles within a narrow mass window [shown in Fig.3a] are used to tag $\eta(\eta')$. The missing $\eta(\eta')$ can be searched for in the distribution of recoil mass of ϕ candidate.

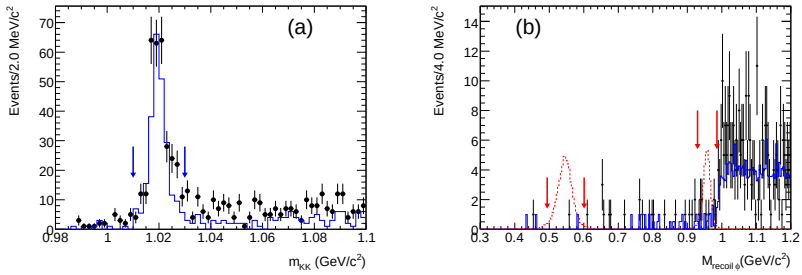

Figure 3: *a) The K^+K^- mass distribution. The arrows indicate the signal region of ϕ candidates. Points with error bars are data; the histogram is expected background. b) Recoil mass distribution against ϕ candidates, M_ϕ^{recoil}, for events within ϕ mass window. Points with error bars are data; the solid histogram is the sum of the expected backgrounds; the dashed histograms (with arbitrary scale) are signals of η and η' invisible decays from MC simulations; the arrows indicate the signal regions of the $\eta(\eta') \to$ invisible.*

The sources of backgrounds are divided into two classes. Class I: The background is from $J/\psi \to \phi\eta(\eta')$, $\phi \to K^+K^-$ and $\eta(\eta')$ decay into visible states. The expected number of background from Class I is 0.18±0.02 (1.0±0.2) in the signal region for $\eta(\eta')$ case. Class II: The background is from J/ψ decays to final states without $\eta(\eta')$ or without both $\eta(\eta')$ and ϕ. For the η invisible decay, the dominant background is from $J/\psi \to \gamma\eta_c$, $\eta_c \to K^\pm\pi^\mp K_L$. For the η' case, the dominant background is from $J/\psi \to \phi K_L K_L$ and $J/\psi \to \phi f_0(980)$, $f_0(980) \to K_L K_L$. The expected number of background from Class II is 0.8 ± 0.2 (9.4 ± 1.7) in the signal region for $\eta(\eta')$ case.

For η case, only one event [shown in Fig.3b] is seen in the η signal region where 1.0 ± 0.2 backgrounds are expected. The upper limit at the 90% C.L. is $N_{UL}^{\eta} = 3.34$ by using the POLE++ program [23] based on Feldman-Cousins Method [22]. For the η' case, an unbinned extended maximum likelihood (ML) fit is performed to the recoil mass distribution against ϕ candidate. The signal

shape in the fit, shown in Fig.4, is driven from data sample of $J/\psi \to \phi\eta'$, $\eta' \to \eta\pi^+\pi^-$, $\eta \to \gamma\gamma$. The shape of dominant background $J/\psi \to \phi f_0(980)$, $f_0(980) \to K_L K_L$, is described from MC simulation [shown in Fig.5], in which the parameters of $f_0(980)$ line shape have been determined in the analysis of $J/\psi \to \phi\pi^+\pi^-$ and ϕK^+K^- from BESII data [24]. The remaining background from $J/\psi \to \phi K_L K_L$ is modeled with a first-order Chebychev polynomial. In the ML fit [shown in Fig.5], the shapes of signal and dominant background are fixed, the numbers of signal yield and backgrounds are float. The upper limit at the 90% C.L. is $N_{UL}^{\eta'} = 10.1$ with Bayesian method.

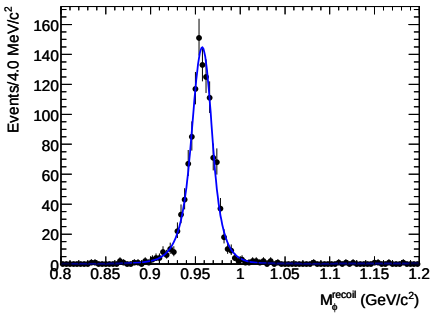

Figure 4: *The M_ϕ^{recoil} distribution for the control sample $J/\psi \to \phi\eta'$, $\eta' \to \pi^+\pi^-\eta(\eta \to \gamma\gamma)$ decay candidates. The solid curve shows the fit results.*

In order to obtain the ratio of $\frac{\mathcal{B}(\eta(\eta')\to\text{invisible})}{\mathcal{B}(\eta(\eta')\to\gamma\gamma)}$, the two-body decays $J/\psi \to \phi\eta(\eta')$, $\eta(\eta') \to \gamma\gamma$ are also studied. The upper limit at the 90% C.L. on the ratio of branching fraction is calculated with

$$\frac{\mathcal{B}(\eta \to \text{invisible})}{\mathcal{B}(\eta \to \gamma\gamma)} < \frac{N_{UL}^{\eta}/\epsilon_\eta}{N_{\gamma\gamma}^{\eta}/\epsilon_{\gamma\gamma}^{\eta}} \frac{1}{1-\sigma_\eta}, \tag{2}$$

where N_{UL}^{η} is the 90% upper limit of the number of observed events for $J/\psi \to \phi\eta$, $\phi \to K^+K^-$, $\eta \to$ invisible decay; ϵ_η is the MC-determined efficiency for the signal channel; $N_{\gamma\gamma}^{\eta}$ is the number of events for the $J/\psi \to \phi\eta$, $\phi \to K^+K^-$, $\eta \to \gamma\gamma$; $\epsilon_{\gamma\gamma}^{\eta}$ is the MC-determined efficiency; and σ_η is the total error for the η case. The upper limit for η' case is obtained similarly.

There is no evidence observed for the invisible decays of η and η', The upper limit at the 90% C.L. on the ratio of $\frac{\mathcal{B}(\eta(\eta')\to\text{invisible})}{\mathcal{B}(\eta(\eta')\to\gamma\gamma)}$ is 2.6×10^{-4} ($2.4 \times$

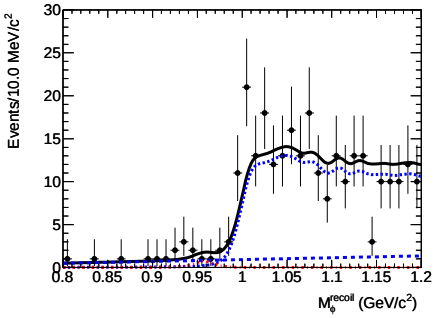

Figure 5: *The M_{ϕ}^{recoil} distribution with events around the η' mass region. Points with error bars are data. The (black) solid curve shows the result of the fit to signal plus background distributions, the (blue) dotted curve shows the background shape from $J/\psi \to \phi f_0(980)(f_0(980) \to K_L K_L)$, the (blue) dashed curve shows the polynomial function for $J/\psi \to \phi K_L K_L$ background, and the (red) dotted-dash curve shows the signal yield.*

10^{-2}) for $\eta(\eta')$ case. Using the branching fraction values of $\mathcal{B}(\eta(\eta') \to \gamma\gamma)$ from the PDG [25], the invisible decays rates are determined to be $\mathcal{B}(\eta \to \text{invisble}) < 1.0 \times 10^{-4}$ and $\mathcal{B}(\eta' \to \text{invisble}) < 5.3 \times 10^{-4}$ at the 90% confidence level. These limits constrain the decays $\eta(\eta') \to UU$, where each U decays invisibly into neutrinos or light dark matter with branching fraction B_{inv}. The resulting $\eta(\eta')$ limits on the U couplings to quarks are improved to be $\sqrt{f_u^2 + f_d^2} < 3 \times 10^{-2}/\sqrt{B_{\text{inv}}}$ and $|f_s| < 4 \times 10^{-2}/\sqrt{B_{\text{inv}}}$, respectively (for $2m_U$ smaller than m_η or $m_{\eta'}$ and not too close to them), f_u, f_d and f_s denoting effective couplings of the U boson to light quarks.

4 Summary

There is no observed signal of light Higgs-like boson A^0 in process $J/\psi \to \gamma A^0$, $A^0 \to \mu^+\mu^-$, based on 106M ψ' data sample. The A^0-mass-dependent upper limits at the 90% C.L. of branching fraction for $J/\psi \to \gamma A^0$, $A^0 \to \mu^+\mu^-$ are range from 4×10^{-7} to 2.1×10^{-5}, for M(A^0) < 3.0 GeV/c^2. There is no obseved signal of light dark matter particles or U boson in invisible decays of η and η', based on 225M J/ψ data sample. The upper limits at the 90% C.L. are determined to be 2.6×10^{-4} for the ratio $\frac{\mathcal{B}(\eta \to \text{invisible})}{\mathcal{B}(\eta \to \gamma\gamma)}$ and 2.4×10^{-2}

for $\frac{\mathcal{B}(\eta' \to \text{invisible})}{\mathcal{B}(\eta' \to \gamma\gamma)}$. These limits may be used to constrain light dark matter particles or spin-1 U bosons.

5 Acknowledgements

We thank the BEPCII group for excellent operation of the accelerator, the IHEP computer group for valuable computing and network support, and all the colleagues contributing on the physical measurements.

References

1. M. Ablikim *et al.* (BESIII Collaboration), Nucl. Instrum. Meth. Methods Phys. Res., Sect. A **614**, 345 (2010).
2. M. Ablikim *et al.* (BESIII Collaboration), Phys. Rev. D **81**, 052005 (2010).
3. M. Ablikim *et al.* (BESIII Collaboration), Chinese Phys. C **36**, 915 (2012).
4. H. K. Park *et al.* (HyperCP Collaboration), Phys. Rev. Lett. **94**, 021801 (2005).
5. D. S. Gorbunov and V. A. Rubakov, Phys. Rev. D **73**, 035002 (2006).
6. J. Ellis, K. Enqvist, and D. Nanopoulos, Phys. Lett. B **147**, 99 (1984); T. Bhattacharya and P. Roy, Phys. Rev. D **38**, 2284 (1988); G. Giudice and R. Rattazzi, Phys. Rep. **322**, 419 (1999).
7. X. G. He, J. Tandean, and G. Valencia, Phys. Rev. Lett. **98**, 081802 (2007).
8. M. Reece and L. T. Wang, J. High Energy Phys. **07**, (2009) 051; M. Pospelov, Phys. Rev. D **80**, 095002 (2009); C.H. Chen, C. Q. Geng, and C.W. Kao, Phys. Lett. B **663**, 400 (2008).
9. R. Dermisek, J. F. Gunion, and B. McElrath, Phys. Rev. D **76**, 051105 (2007).
10. C. Edwards *et al.*, (Crystal Ball Collaboration), Phys. Rev. Lett. bf 48, 903 (1982).
11. K. Nakamura *et al.*, (Particle Data Group), J. Phys. G **37**, 075021 (2010).

12. P. Fayet, Phys. Lett. B **675**, 267 (2009).

13. B. McElrath, arXiv:0712.0016[hep-ph], *Proceedings of the CHARM 2007 Workshop*, Ithaca, NY, August 5-8, 2007.

14. P. Fayet, Phys. Rev. D **81**, 054025 (2010).

15. P. Fayet, Phys. Rev. D **74**, 054034 (2006).

16. P. Fayet, Nucl. Phys. B **347**, 743 (1990).

17. A. V. Artamonov *et al.* (E949 Collaboration), Phys. Rev. D **72**, 091102 (2005).

18. M. Ablikim *et al.* (BES Collaboration), Phys. Rev. Lett. **97**, 202002 (2006).

19. P. Naik *et al.* (CLEO Collaboration), Phys. Rev. Lett. **102**, 061801 (2009).

20. M. Ablikim *et al.* (BES Collaboration), Phys. Rev. Lett. **100**, 192001 (2008).

21. B. Aubert *et al.* (BABAR Collaboration), Phys. Rev. Lett. **103**, 251801 (2009); P. Rubin *et al.* (CLEO Collaboration), Phys. Rev. D **75**, 031104 (2007); O. Tajima *et al.* (Belle Collaboration), Phys. Rev. Lett. **98**, 132001 (2007).

22. G. J. Feldman and R. D. Cousins, Phys. Rev. D **57**, 3873 (1998).

23. J. Conrad, O. Botner, A. Hallgren and C. Peréz de los Heros, Phys. Rev. D **67**, 012002 (2003); http://polepp.googlecode.com/svn/tags/POLEPP-1.1.0.

24. M. Ablikim *et al.* (BES Collaboration), Phys. Lett. B **607**, 243 (2005).

25. J. Beringer *et al.* (Particle Data Group), Phys. Rev. D **86**, 010001 (2012).